Intestinal monocytes and macrophages are required for T cell polarization in response to *Citrobacter rodentium*

Heidi A. Schreiber,[1] Jakob Loschko,[1] Roos A. Karssemeijer,[2] Amelia Escolano,[1] Matthew M. Meredith,[1] Daniel Mucida,[2] Pierre Guermonprez,[1,4] and Michel C. Nussenzweig[1,3]

[1]Laboratory of Molecular Immunology, [2]Mucosal Immunology and [3]Howard Hughes Medical Institute, The Rockefeller University, New York, NY 10065
[4]Laboratory of Phagocyte Immunobiology, Center for Molecular and Cellular Biology of Inflammation, Peter Gorer Department of Immunobiology, Division of Immunology, Infection and Inflammatory Disease, King's College, London SE5 8AN, UK

Dendritic cells (DCs), monocytes, and macrophages are closely related phagocytes that share many phenotypic features and, in some cases, a common developmental origin. Although the requirement for DCs in initiating adaptive immune responses is well appreciated, the role of monocytes and macrophages remains largely undefined, in part because of the lack of genetic tools enabling their specific depletion. Here, we describe a two-gene approach that requires overlapping expression of *LysM* and *Csf1r* to define and deplete monocytes and macrophages. The role of monocytes and macrophages in immunity to pathogens was tested by their selective depletion during infection with *Citrobacter rodentium*. Although neither cell type was required to initiate immunity, monocytes and macrophages contributed to the adaptive immune response by secreting IL-12, which induced Th1 polarization and IFN-γ secretion. Thus, whereas DCs are indispensable for priming naive CD4$^+$ T cells, monocytes and macrophages participate in intestinal immunity by producing mediators that direct T cell polarization.

CORRESPONDENCE
Michel Nussenzweig:
nussen@rockefeller.edu

Abbreviations used: CDC, conventional DC; CDP, common DC progenitor; LysM, lysozyme; MDP, macrophage–DC progenitor; mLN, mesenteric LN.

Inducing specific immunity and maintaining tolerance requires cells of the mononuclear phagocyte lineage. This lineage is comprised of three closely related cell types: DCs, monocytes, and macrophages (Shortman and Naik, 2007; Geissmann et al., 2010a,b; Liu and Nussenzweig, 2010; Yona and Jung, 2010; Chow et al., 2011). DCs are essential to both immunity and tolerance (Steinman et al., 2003); however, the role monocytes and macrophages play in these processes is not as well defined (Geissmann et al., 2008).

In mice, DCs and monocytes arise from the same hematopoietic progenitor, known as the macrophage–DC progenitor (MDP; Fogg et al., 2006). Their development diverges when MDPs become either common DC progenitors (CDPs) that are Flt3L-dependent, or monocytes, which are dependent on CSF1 (M-CSF; Witmer-Pack et al., 1993; McKenna et al., 2000; Fogg et al., 2006; Waskow et al., 2008). CDPs develop into either plasmacytoid DCs or preDCs that leave the bone marrow to seed lymphoid and nonlymphoid tissues, where they further differentiate into conventional DCs (cDCs; Liu et al., 2009). In contrast, monocytes circulate in the blood and through tissues, where they can become activated and develop into several different cell types, including some but not all tissue macrophages (Schulz et al., 2012; Serbina et al., 2008; Yona et al., 2013).

Despite their common origin from the MDP, steady-state lymphoid tissue cDCs can be distinguished from monocytes or macrophages by expression of cell surface markers. For example, cDCs in lymphoid tissues express high levels of CD11c and MHCII, but lack the expression of CD115 and F4/80 found in monocytes and macrophages, respectively. However, this distinction is far more difficult in peripheral

H.A. Schreiber and J. Loschko contributed equally to this paper.
P. Guermonprez and M.C. Nussenzweig contributed equally to this paper.

The Rockefeller University Press $30.00
J. Exp. Med. 2013 Vol. 210 No. 10 2025-2039
www.jem.org/cgi/doi/10.1084/jem.20130903

The Journal of Experimental Medicine

tissues, like the intestine or lung, or during inflammation when monocytes begin to express many features of DC including high levels of MHCII and CD11c (Serbina et al., 2003; León et al., 2007; Hashimoto et al., 2011).

The function of cDCs in immunity and tolerance has been explored extensively using a series of different mutant mice to ablate all or only some subsets of cDCs (Jung et al., 2002; Liu and Nussenzweig, 2010; Chow et al., 2011). In contrast, the methods that are currently available to study the function of monocytes and macrophages in vivo are far more restricted and less specific (Wiktor-Jedrzejczak et al., 1990; Dai et al., 2002; MacDonald et al., 2010; Chow et al., 2011). For example, *Ccr2*$^{-/-}$ and *Ccr2*^{DTR} mice (Boring et al., 1997; Kuziel et al., 1997; Serbina and Pamer, 2006; Tsou et al., 2007) have been used to study monocytes (Boring et al., 1997; Peters et al., 2004; Hohl et al., 2009; Nakano et al., 2009). However, CCR2 is also expressed on some subsets of cDCs, activated CD4$^+$ T cells, and NK cells (Kim et al., 2001; Hohl et al., 2009; Egan et al., 2009; Zhang et al., 2010). Thus, it is challenging to dissect the precise role of monocytes as opposed to other cell types in immune responses in *Ccr2*$^{-/-}$ or *Ccr2*^{DTR} mice. Inducible DTR expression in CD11c^{Cre} x CX$_3$CR1$^{LsL\text{-}DTR}$ mice is far more specific (Diehl et al., 2013), but restricted to a small subset of mononuclear phagocytes.

Here, we describe a genetic approach to targeting monocytes and macrophages that spares cDCs and lymphocytes, and we compare the effects of monocyte and macrophage ablation to cDC depletion on the adaptive immune response to intestinal infection with *Citrobacter rodentium*.

RESULTS

Lysm^{Cre} *X Csf1r*$^{LsL\text{-}DTR}$ mice

To target monocytes and macrophages in vivo, we combined two genes, the macrophage colony-stimulating factor receptor (M-CSF-R; *Csf1r*; CD115) and lysozyme (*Lyz2*; LysM), neither of which alone is entirely specific for these cells. Transgenic mice that carry a BAC encoding a human diphtheria toxin receptor–mCherry fusion protein (DTR-mCherry) preceded by a loxP-flanked transcriptional Stop element under the control of the Csf1r promoter (*Csf1r*$^{LsL\text{-}DTR}$ mice; Fig. 1 A) were crossed with mice that express Cre recombinase under the control of *LysM* (Lysm^{Cre}; Clausen et al., 1999). LysM-expressing cells in *Lysm*^{Cre} *x Csf1r*$^{LsL\text{-}DTR}$ mice (hereafter MM^{DTR} mice, for monocyte and macrophage), delete the Stop element, which permits transcription of DTR-mCherry specifically in LysM/Csf1r double-positive cells. To verify DTR-mCherry expression in monocytes but not cDCs in MM^{DTR} mice, we examined spleen cells by flow cytometry (Fig. 1 B). We found that Ly6C^{high}CD115$^+$ spleen monocytes uniformly expressed mCherry, whereas MHCII^{high}CD11c^{high} cDCs did not (Fig. 1 B). Thus, DTR-mCherry is expressed in monocytes but not cDCs in the spleen of MM^{DTR} mice.

To test for deletion, we injected MM^{DTR} mice with 4 ng of diphtheria toxin (DT) per gram of body weight (~100 ng per mouse). A single DT injection resulted in the complete loss of peripheral blood and bone marrow monocytes after 24 h (Ly6C^{high} and Ly6C^{low}; Fig. 1 C). Peripheral blood Ly6C^{high} monocytes returned to normal levels after 3 d and were present at super-physiological levels in blood on days 4 and 5 before returning to baseline after 6 d (Fig. 1 D). Consistent with their proposed precursor product relationship (Yona et al., 2013), Ly6C^{low} monocyte reconstitution lags behind that of the Ly6C^{high} population (Fig. 1 D). The increase in peripheral blood monocytes was associated with an 18-fold increase in the serum concentration of M-CSF 24 h after DT injection (Fig. 1 E). In contrast, serum concentrations of GM-CSF and Flt3L remained unchanged (unpublished data). We conclude that DT injection into MM^{DTR} mice results in efficient ablation of peripheral blood monocytes.

Macrophages and inflammatory monocytes

To examine the specificity of ablation in MM^{DTR} mice, we compared these mice with zDC^{DTR} (Meredith et al., 2012) and CD11c^{DTR} mice (Jung et al., 2002). Because DT injection is fatal for zDC^{DTR} and CD11c^{DTR} mice, we produced bone marrow chimeras for all three strains, as well as B6 controls. As expected, DT injection did not affect cDCs (CD11c$^+$MHCII^{high}) in MM^{DTR} or B6 controls, but ablated these cells in both zDC^{DTR} and CD11c^{DTR} chimeras (Fig. 2 A). In contrast, all spleen monocytes (CD115$^+$Ly6C^{high}) were ablated in MM^{DTR} mice (Fig. 2 A), but not in zDC^{DTR} mice. Finally, steady-state T and B lymphocytes were unaffected by DT injection in MM^{DTR} mice (Fig. 2 B). We conclude that DT injection depletes monocytes, but not cDCs or lymphoid cells, in MM^{DTR} mice.

Monocytes can develop many of the features of cDCs under inflammatory conditions (Serbina et al., 2003; León et al., 2007; Hohl et al., 2009). For example, during infection with *Listeria monocytogenes*, monocytes develop into Tip DCs that express high levels of CD11c and MHCII and produce both TNF and iNOS (Serbina et al., 2003). However, despite their phenotypic resemblance to cDCs, these activated monocytes are depleted by DT injection in MM^{DTR} but not in zDC^{DTR} mice (Fig. 2 C; Meredith et al., 2012).

In addition to monocytes, tissue macrophages also express both LysM and Csf1r. To determine if splenic macrophages are deleted by DT injection in MM^{DTR} mice, we examined spleen sections by immunofluorescence (Hashimoto et al., 2011) using antibodies to identify red pulp (F4/80^{high}), marginal zone (SIGNR1$^+$), and marginal zone metallophilic (CD169$^+$) macrophages. All three macrophage populations were entirely ablated by 24 h after DT injection (Fig. 2 D). Red pulp, peritoneal, lung alveolar and interstitial macrophages, and Kupffer cells were also depleted 24 h after DT injection in MM^{DTR} mice (Fig. 2 E).

We conclude that a two-gene approach that relies on both LysM and Csf1r gene expression results in specific ablation of monocytes, macrophages, and inflammatory monocytes, and does not affect conventional splenic DCs or lymphocytes.

DCs, monocytes, and macrophages in the intestine

The phenotype of immune cells in the intestine is altered in part by their exposure to commensal bacteria. As a result,

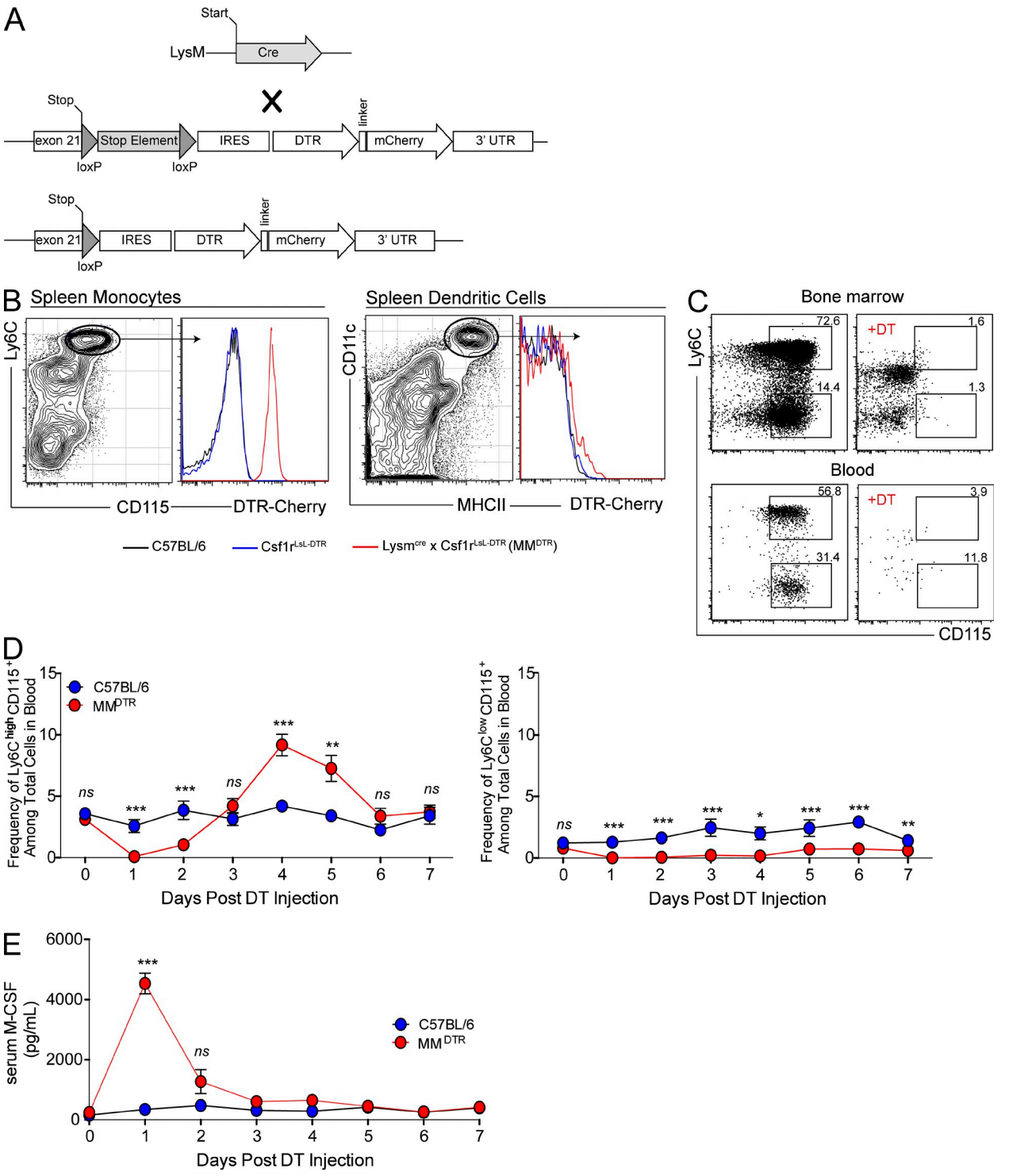

Figure 1. MM^{DTR} mice. (A) Diagrammatic representation of *Lysm*^{cre} (top) *Csf1r*$^{LsL\text{-}DTR}$ (middle) and MM^{DTR} (bottom) mice. Expression of Cre recombinase is under the control of LysM. Expression of a DTR-mCherry protein in BAC transgenic mice is under the control of CSF1R, but is inhibited by a loxp site-flanked Stop element. In MM^{DTR} mice, CSF1R-expressing cells that had expressed LysM express the DTR-mCherry fusion protein and can be deleted by DT. (B) Flow cytometric analysis of mCherry expression on splenic monocytes (Lin^{neg}CD11b^{high}Ly6C^{high}CD115^{+}) and cDCs (Lin^{neg}CD11c^{high}MHCII^{high}). Lineage gating includes NK1.1, B220, CD19, Ly6G, and TCRβ. (C) Flow cytometry plots of bone marrow (top) and peripheral blood (bottom) without (left) and 24 h after (right) DT injection. Cells gated on Lin^{neg}CD11b^{high}Ly6G^{neg}. (D) Monocyte abundance in peripheral blood at multiple time points after DT injection in B6 and MM^{DTR} mice. Percentage of the two major monocyte populations, Lin^{neg}CD11b^{high}CD115^{+}Ly6C^{high} (left) and Lin^{neg}CD11b^{high}CD115^{+}Ly6C^{low} (right) in the blood. (E) M-CSF concentrations in sera of DT-treated MM^{DTR} mice determined by ELISA at multiple time points after DT injection. Results represent two to three experiments with two to five mice per group and experiment. Error bars indicate SEM. *, $P < 0.05$; **, $P < 0.01$; ***, $P < 0.001$.

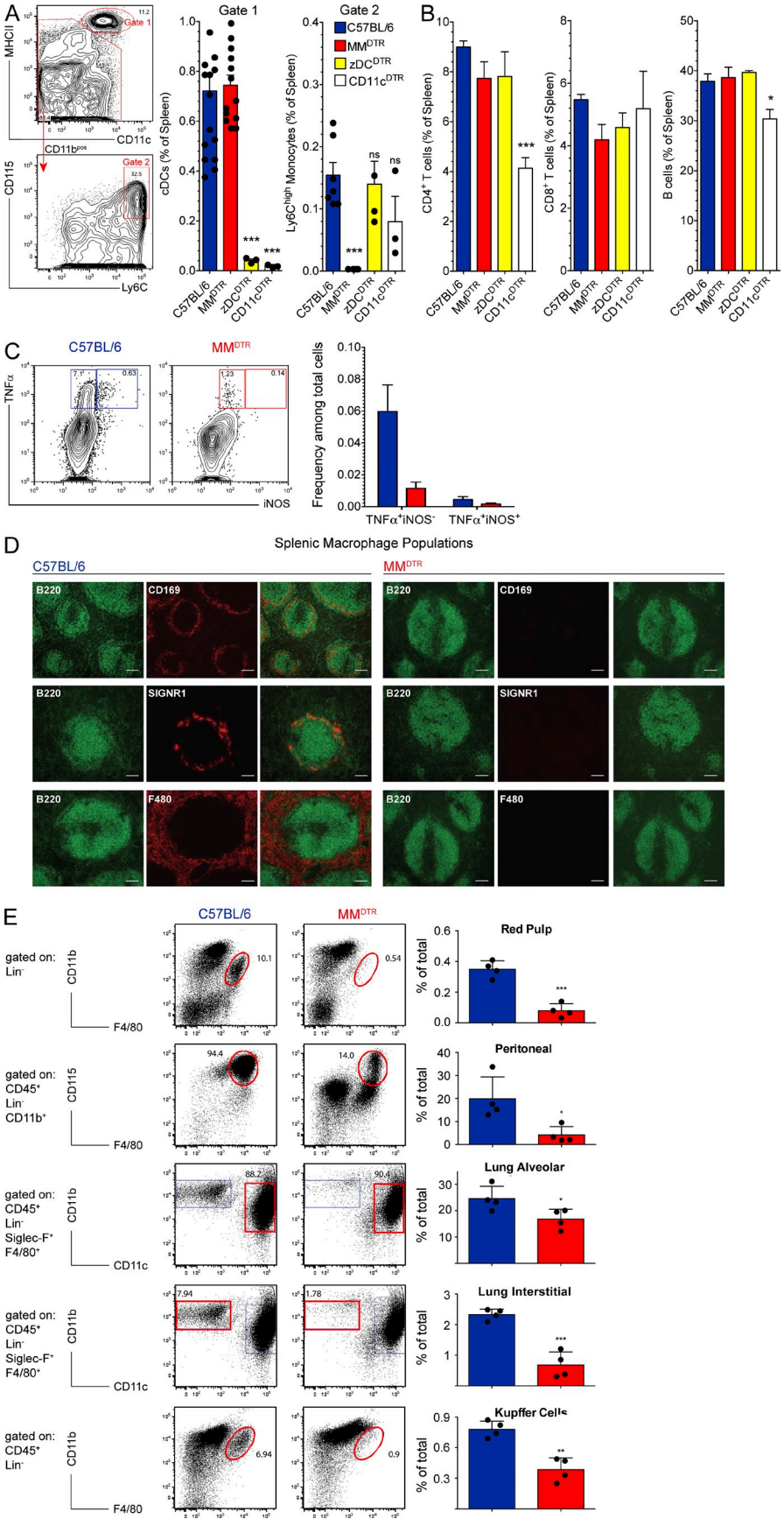

Figure 2. Depletion of monocytes, macrophages, and cDCs in CD11c^{DTR}, zDC^{DTR}, and MM^{DTR} mice. (A) Flow cytometry plots of spleen cDCs (Gate 1, CD11c^{high}MHCII^{high}, gated on Lin^{neg}) and monocytes (Gate 2, Ly6C^{high}CD115^{+}, gated on Lin^{neg}MCHII^{low} CD11c^{low}CD11b^{+}). Bar graphs show percentage of cDCs and monocytes among total spleen cells 24 h after DT injection. Each data point corresponds to an individual mouse. (B) Bar graphs show percentage of CD4^{+} and CD8^{+} T and B lymphocytes among total spleen cells 24 h after DT injection. Results represent three mice per group. (C) Intracellular staining for TNF and iNOS in splenic monocytes from DT-injected B6 and MM^{DTR} mice infected with *L. monocytogenes*. Gated on Lin^{neg}CD11b^{high} MHCII$^{low\text{-}int}$CD11c$^{low\text{-}int}$ cells. Cells were stimulated ex vivo with heat-killed *L. monocytogenes*. Results represent two to three experiments with two to five mice per group and experiment. (D) Spleens from B6 and MM^{DTR} mice 24 h after DT injection. Sections were stained with B220 (green) to visualize B cell zones and macrophage markers (red) to reveal metallophilic (CD169), marginal zone (SIGNR1), and red pulp (F4/80) macrophages. Bars, 100 µm. (E) Tissue macrophage depletion in B6 and MM^{DTR} mice 24 h after DT injection. Results from one representative experiment with four mice per group. Error bars indicate SEM. *, $P < 0.05$; **, $P < 0.01$; ***, $P < 0.001$.

monocytes and macrophages acquire some of the features of cDCs including high levels of MHCII and CD11c expression, making it difficult to distinguish the two cell types (Bogunovic et al., 2012; Varol et al., 2010). To examine the origin of DC-like cells in the small intestine lamina propria and serosa, we compared bone marrow chimeras of B6 control, MM^{DTR}, zDC^{DTR}, and $CD11c^{DTR}$ mice injected with DT. 18–24 h after injection, single-cell suspensions from the small intestine lamina propria or serosa/muscularis were analyzed by flow cytometry (Fig. 3 A). Cells that resembled DCs, due to their high-level expression of CD11c and MHCII, were further fractionated by CD103 (integrin αE) and CD11b expression (Bogunovic et al., 2009; Varol et al., 2010).

$CD103^+CD11b^-$ lamina propria cells, which originate from preDCs (Bogunovic et al., 2009; Varol et al., 2009), were depleted in zDC^{DTR} and $CD11c^{DTR}$, but not in MM^{DTR} mice (Fig. 3, A and B). Conversely, $CD103^-CD11b^+$ cells, which are largely derived from peripheral blood $Ly6C^{high}$ monocytes in the steady-state and during inflammation (Varol et al., 2007, 2009; Bogunovic et al., 2009; Yona et al., 2013), were significantly depleted in MM^{DTR} and $CD11c^{DTR}$, but minimally depleted in zDC^{DTR} mice. This $F4/80^+$ population remains partially depleted for 4 d after DT injection in MM^{DTR} mice, but returns to a steady-state frequency by 1 wk (Fig. 3 C). Thus, $CD103^+CD11b^-$ and $CD103^-CD11b^+$ cells in the lamina propria are preDC and monocyte-derived, respectively. In contrast, the $CD103^+CD11b^+$ population was partially depleted in both zDC^{DTR} and MM^{DTR} mice (Fig. 3, A and B). We conclude that $CD103^+CD11b^+$ lamina propria cells are a heterogeneous population containing cDCs as well as monocyte/macrophages.

In the serosa/muscularis, a layer of the gut distant from the lumen, $MHCII^+CD11c^{int}$ cells were homogeneously $CD103^-CD11b^+$, and these cells were depleted in MM^{DTR} and $CD11c^{DTR}$ but not zDC^{DTR} mice (Fig. 3, D and E).

Cells migrating from the lamina propria are preDC derived

Lamina propria $CD103^+CD11b^+$ cells migrate to LNs in a CCR7-dependent fashion and facilitate antigen transport during infection (Bogunovic et al., 2009). To determine the origin of the migrating $CD103^+CD11b^+$ cells, we examined steady-state migratory populations of mesenteric lymph node DCs after DT injection (Fig. 4, A and B). In contrast to the lamina propria, all $CD103^+CD11b^-$ and $CD103^+CD11b^+$ cells were depleted in the mesenteric lymph node after DT injection in zDC^{DTR} and $CD11c^{DTR}$ mice, but these cells were not altered in MM^{DTR} mice. In accordance with this finding, $CD103^+CD11b^+$ cells remaining in the lamina propria of MM^{DTR} mice after DT injection expressed high levels of CCR7 mRNA, whereas those in zDC^{DTR} mice showed reduced low levels of CCR7 mRNA (Fig. 4 C). We conclude that in steady state, only preDC-derived $CD103^+CD11b^+$ cells migrate from the lamina propria to the mesenteric lymph node.

To determine whether infection-induced inflammation altered the composition of these migratory populations, we examined mesenteric lymph node DCs 3 d after oral infection with *C. rodentium*, an enteric pathogen that resembles enteropathogenic and enterohemorrhagic *E. coli* (Mundy et al., 2005). Again, both $CD103^+CD11b^-$ and $CD103^+CD11b^+$ migratory DCs in the mesenteric LN (mLN) were entirely depleted in zDC^{DTR}, but not altered in MM^{DTR} mice depleted of monocytes and macrophages (Fig. 4, D and E). Furthermore, when the number of living bacteria in the draining mLN was determined, a strong, albeit not statistically significant decrease in CFU was observed, indicating that the transport of *C. rodentium* from the intestinal lumen to the mLN is not as efficient in zDC^{DTR} mice as it is in control animals. This trend was, however, not observed in MM^{DTR} mice (Fig. 4 F).

To test whether the impaired antigen transport observed in zDC^{DTR} mice had an effect on T cell priming, we measured OT-II $CD4^+$ T cell proliferation and CD62L down-regulation after infection with OVA-expressing *C. rodentium*. We observed significantly less T cell proliferation and CD62L down-regulation in zDC^{DTR} mice compared with B6 mice (Fig. 4, G–I). Furthermore, the observation that T cell priming (proliferation and down-regulation of CD62L) still occurred in MM^{DTR} mice correlates with CFU data suggesting that monocytes and macrophages are not involved in antigen transport and their absence has no influence on priming naive T cells in the draining LN.

We conclude that in the steady state and during infection, only preDC-derived $CD103^+CD11b^-$ and $CD103^+CD11b^+$ cells migrate from the lamina propria to the mesenteric lymph node. Furthermore, priming of T cells is only impaired in the absence of preDC-derived migratory DCs, and therefore, monocyte-derived cells are not involved in antigen transport or priming of naive T cells.

Monocytes and macrophages in intestinal infection

To examine the role of monocytes and macrophages in adaptive immune responses in the intestine, we repeatedly injected DT starting 1 d before *C. rodentium* infection and every other day thereafter. Monocyte- and macrophage-depleted MM^{DTR} and cDC-depleted zDC^{DTR} mice experienced significant weight loss when compared with B6 controls (Fig. 5 A). Consistent with the weight loss, all zDC^{DTR} mice succumbed to infection, with a mean survival of 11 d (Fig. 5 B). In contrast, although monocyte- and macrophage-depleted mice were more susceptible than controls, the difference was not statistically significant (Fig. 5 B). Thus, whereas loss of cDCs led to weight loss and a fatal infection, monocyte- and macrophage-depleted mice lost weight initially, but infection was only fatal in 50% of all MM^{DTR} mice infected with *C. rodentium*. The number of fecal and invasive liver colony-forming units of *C. rodentium* in DT-treated mice at day 9 mirrored survival in that zDC^{DTR} mice showed the highest levels, followed by MM^{DTR} mice (Fig. 5, C and D). We conclude that cDCs are essential to the immune response against *C. rodentium* and for controlling bacterial dissemination.

Monocytes and macrophages in adaptive immunity to an intestinal pathogen

Infection with *C. rodentium* is associated with both an IL-22–driven innate response (Satoh-Takayama et al., 2008; Zheng

et al., 2008; Ota et al., 2011; Sonnenberg et al., 2011; Tumanov et al., 2011; Basu et al., 2012) and the induction of Th17 and Th1 CD4$^+$ adaptive immune responses (Higgins et al., 1999; Bry and Brenner, 2004; Bry et al., 2006; Simmons et al., 2002; Mundy et al., 2005; Mangan et al., 2006). To measure the CD4$^+$ T cell response during infection, lamina propria cells

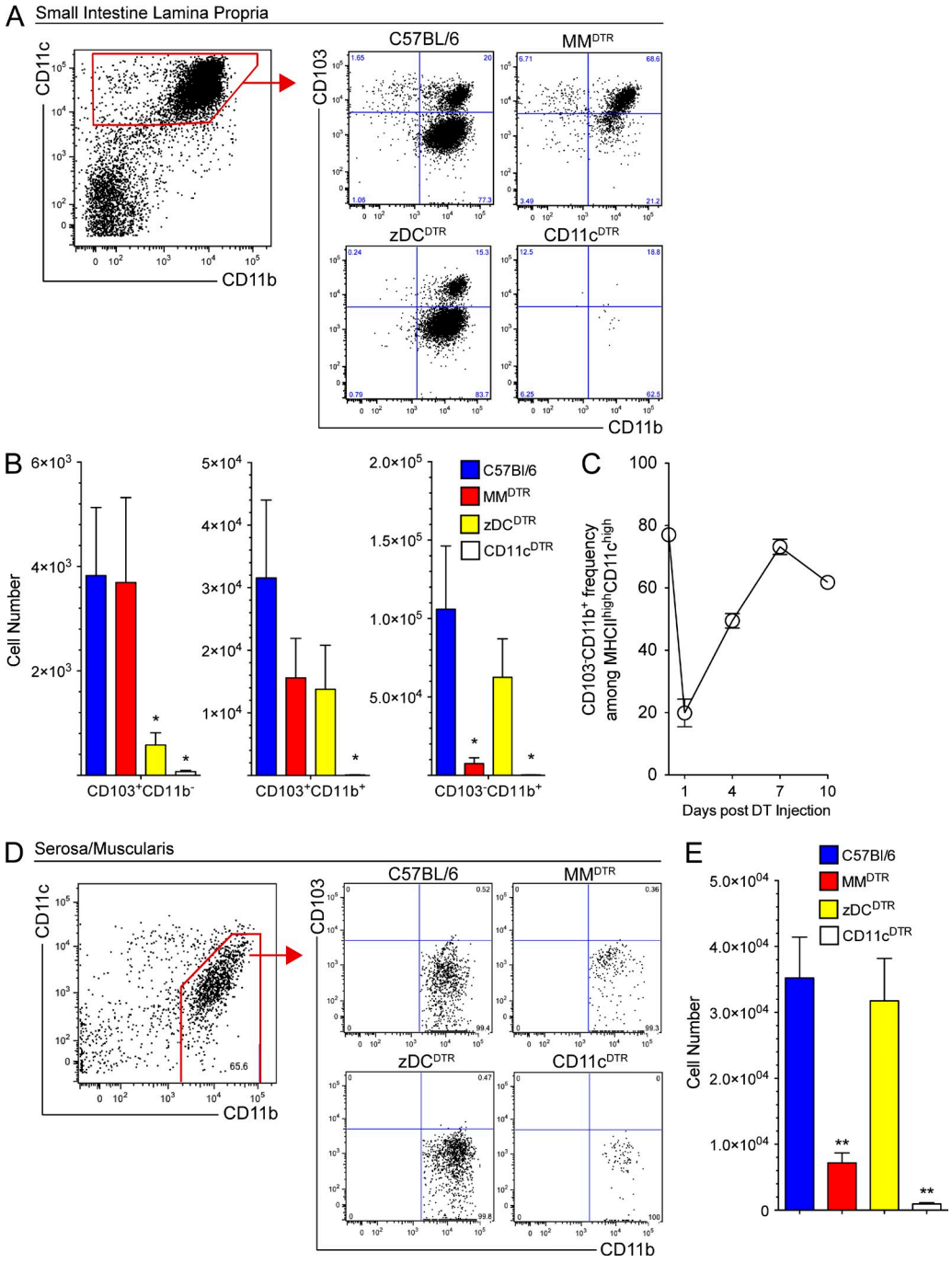

Figure 3. Depletion of monuclear phagocytes in the intestine of MM^{DTR}, zDC^{DTR}, and CD11c^{DTR} mice. (A) Flow cytometry plots of small intestine lamina propria mononuclear phagocyte populations 24 h after DT injection in chimeric B6, MM^{DTR}, zDC^{DTR}, and CD11c^{DTR} mice. Gating on Lin^{neg}CD45$^+$MHCII^{high} (left) and CD103 versus CD11b plots on gated population for each genotype (right). (B) Bar graphs show absolute numbers of CD103$^+$CD11b$^-$, CD103$^+$CD11b$^+$, and CD103$^-$CD11b$^+$ cells in the small intestine lamina propria. Data pooled from >3 experiments with 3–17 mice per group. (C) Reconstitution of macrophage after single DT injection. Frequency of CD103$^-$CD11b$^+$ cells among total MHCII^{high}CD11c^{high} cells at several time points after DT injection. Each time point consists of three mice per group. (D) Flow cytometry plots of isolated serosa/muscularis cells 24 h after DT injection in chimeric B6, MM^{DTR}, zDC^{DTR}, and CD11c^{DTR}. Gating on CD11c$^{low\text{-}int}$CD11b$^+$ (left) and CD103 versus CD11b on gated population (right). (E) Bar graphs show absolute numbers of CD103$^-$CD11b$^+$ cells in the serosa/muscularis. Results represent two experiments with 2–5 mice per group and experiment. Error bars indicate SEM. *, $P < 0.05$; **, $P < 0.01$.

were restimulated ex vivo and stained for IFN-γ and IL-17. Compared with B6 controls, cDC-depleted zDC^{DTR} mice displayed an overall decrease in activated T cells and a lower frequency of IFN-γ– or IL-17–producing cells (Fig. 5, E and F). The frequency of IFNγ– and IL-17–producing CD4^{+} cells observed in depleted zDC^{DTR} mice was similar to that in naive mice (unpublished data). This reflects our finding, that there is little or no CD4^{+} T cell priming in the absence

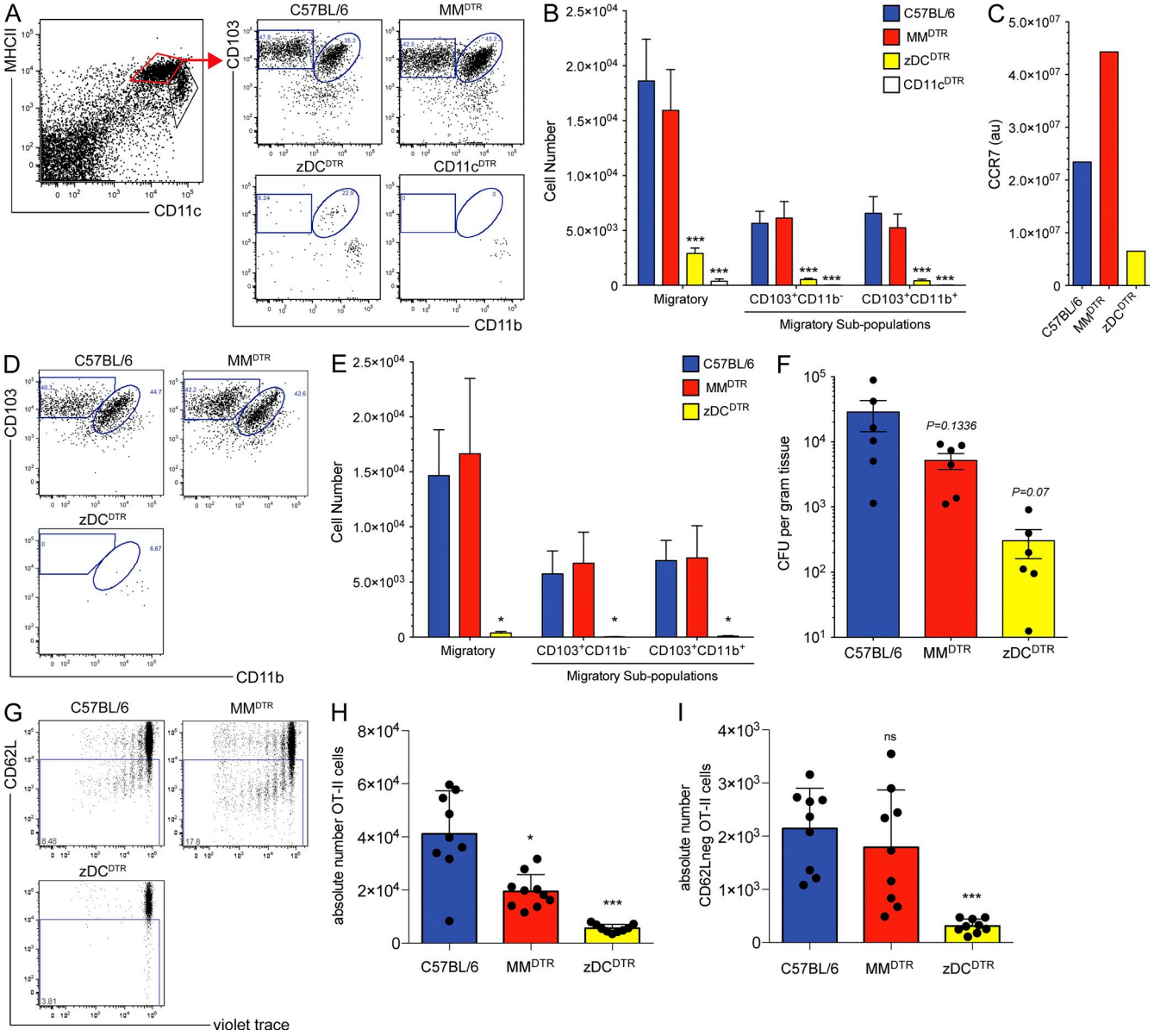

Figure 4. Migratory cells in mesenteric lymph nodes after DT injection in CD11c^{DTR}, zDC^{DTR}, and MM^{DTR} mice. (A) Flow cytometry plots of mesenteric LN DCs 24 h after DT injection in B6, MM^{DTR}, zDC^{DTR}, and CD11c^{DTR} mice. Gating on Lin^{neg}CD11c^{+}MHCII^{high} cells (left) and CD103 versus CD11b staining on the gated population (right). (B) Bar graphs show absolute number of CD11c^{+}MHCII^{high} total migratory cells, and CD103^{-}CD11b^{+} and CD103^{+}CD11b^{+} subsets. Data pooled from >3 experiments, 8–10 mice per group. (C) CCR7 transcript levels determined by quantitative real-time PCR from FACS-sorted lamina propria CD103^{+}CD11b^{+} cells 24 h after DT injection in B6 (blue), MM^{DTR} (red), and zDC^{DTR} (yellow) mice. (D) Flow cytometry plots of mesenteric LN DCs 3 d after *C. rodentium* infection in DT-injected B6, MM^{DTR}, and zDC^{DTR} mice. (E) Bar graphs show absolute number of CD11c^{+}MHCII^{high} total migratory cells, and CD103^{-}CD11b^{+} and CD103^{+}CD11b^{+} subsets. Results represent two experiments with three mice per group and experiment. Error bars indicate SEM. (F) CFU per gram of homogenized mesenteric lymph node tissue 3 d after *C. rodentium* infection. Each data point corresponds to an individual mouse from two independent experiments. Error bars indicate SEM. (G–I) 5 × 10^{6} OT-II cells labeled with violet trace were transferred to DT-treated B6, zDC^{DTR}, and MM^{DTR} mice. Mice were infected with an OVA-expressing strain of *C. rodentium* the next day. 5 d after the infection, T cell proliferation (dilution of violet trace) and activation (down-regulation of CD62L) were determined in the mLN. (G) Dilution of violet trace cell division dye and down-regulation of CD62L. Shown are representative plots from two independent experiments with 4–5 mice per group and experiment. Bar graphs show absolute numbers of (H) total OT-II cells and (I) CD62L low OT-II cells. *, P < 0.05; **, P < 0.01; ***, P < 0.001.

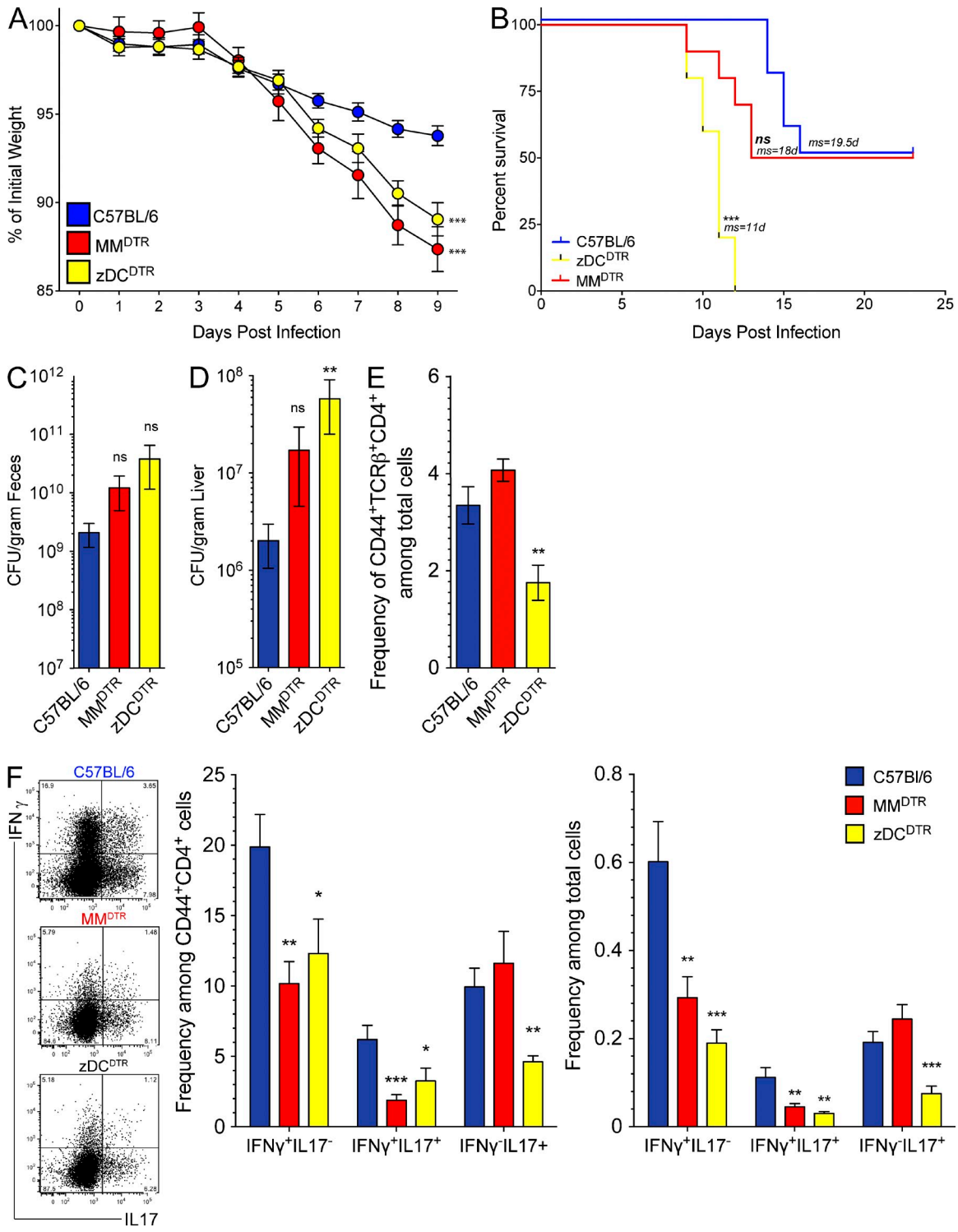

Figure 5. Response to *C. rodentium* infection in MM^{DTR} and zDC^{DTR} mice. (A) Weight loss after infection with *C. rodentium*. B6, MM^{DTR}, and zDC^{DTR} mice received DT 1 d before infection and then every other day for 9 d. Each group contains 24–32 mice. (B) Percent of mice surviving *C. rodentium* infection. As in A, but mice were observed for survival for 23 d. Mean survival (ms) for each group is indicated. Each group contains 6–10 mice. (C) CFU per gram of homogenized feces at day 9 after infection. (D) CFU per gram of homogenized liver at day 9 after infection. (E) Frequency of TCRβ$^+$CD4$^+$CD44$^+$ cells (obtained from Lin$^-$CD45$^+$ gate) among total colonic lamina propria cells. (F) Flow cytometry plots from colonic lamina propria cells isolated 9 d after *C. rodentium* infection. Cells were stimulated ex vivo with PMA/Ionomycin and stained for IFN-γ and IL-17. Representative plots show Lin^{neg}CD45$^+$TCRβ$^+$CD4$^+$CD44^{high} cells. Bar graphs show frequency of IFN-γ$^+$IL-17$^-$, IFN-γ$^+$IL-17$^+$, and IFN-γ$^-$IL-17$^+$ subsets among CD4$^+$CD44^{high} colonic lamina propria cells. Data pooled from >3 experiments, 10–18 mice per group. *, $P < 0.05$; **, $P < 0.01$; ***, $P < 0.001$. Error bars indicate SEM.

of cDCs in DT-treated, *C. rodentium*–infected zDC^{DTR} mice (Fig. 4, G–I).

In contrast, MM^{DTR} mice showed normal frequencies of activated T cells in the lamina propria, but fewer cells producing IFN-γ or the combination of IFN-γ and IL-17, whereas the frequency of cells producing IL-17 alone were not affected (Fig. 5, E and F). Thus, intestinal monocytes and macrophages contribute to the IFN-γ-CD4 T cell response after infection with *C. rodentium*. Similarly, monocyte and macrophage depletion after *Listeria monocytogenes* infection led to decreased survival and less IFN-γ production in antigen-specific CD4$^+$ T cells, despite equal T cell activation compared with B6 controls (Fig. 6, A–C). We conclude that monocytes and macrophages shape the adaptive immune response to *C. rodentium* and *L. monocytogenes* by supporting the development of IFN-γ–producing Th1 cells.

Complete Th1 differentiation during intestinal bacterial infection requires high-level expression of IL-12 and IFN-γ (Higgins et al., 1999; Simmons et al., 2002). Because monocyte and macrophage depletion altered Th1 immunity, we tested whether their depletion plays a direct role in the induction of Th1 immunity by IL-12 production. On a per cell basis, cDCs produce far higher amounts of IL-12 during inflammation than monocytes and macrophages (Heufler et al., 1996; Gorak et al., 1998; Fig. 7 A); however, the latter are a more abundant population in the intestines (Lee et al., 1985; Fig. 3 A). IL12p70 cytokine production in colonic tissue was measured 3 d after *C. rodentium* infection in DT-treated B6 control and MM^{DTR} mice (Fig. 7 B). Consistent with their tissue distribution, we found a large decrease in the overall intestinal IL12p70 protein level in *C. rodentium* infected mice depleted of monocytes and macrophages (Fig. 7 B). IL-12–induced differentiation of Th1 cells requires activation and phosphorylation of the transcription factor Stat4 (Hsieh et al., 1993; Murphy et al., 2000; Athie-Morales et al., 2004). To determine whether the monocyte and macrophage-induced reduction in local IL-12 was responsible for the observed decrease in IFN-γ production, we measured phosphorylation of Stat4 on tyrosine 693 in activated CD4$^+$ T cells within the lamina propria at day 9 of infection (Fig. 7 C). Compared with controls, DT injection in *C. rodentium*–infected, MM^{DTR}-treated mice resulted in significantly less Stat4 phosphorylation. We conclude that intestinal monocytes and macrophages contribute to the production of the IL-12 that is required for Th1 cell polarization in the intestinal lamina propria during infection.

DISCUSSION

Although it is well established that cells of the mononuclear phagocyte lineage are essential for both innate and adaptive immunity (Steinman et al., 2003; Liu and Nussenzweig, 2010; Yona and Jung, 2010; Chow et al., 2011), understanding their individual contributions to immunity has been difficult because of overlapping phenotypic features and a lack of specific genetic tools (Lewis et al., 2011; Langlet et al., 2012; Miller et al., 2012; Tamoutounour et al., 2012). Here, we describe a two-gene approach to target monocytes and macrophages but not cDCs.

Genetic experiments, beginning with deletion of cDCs in CD11c^{DTR} mice (Jung et al., 2002), established that cDCs are required for T cell priming in vivo (Bennett and Clausen,

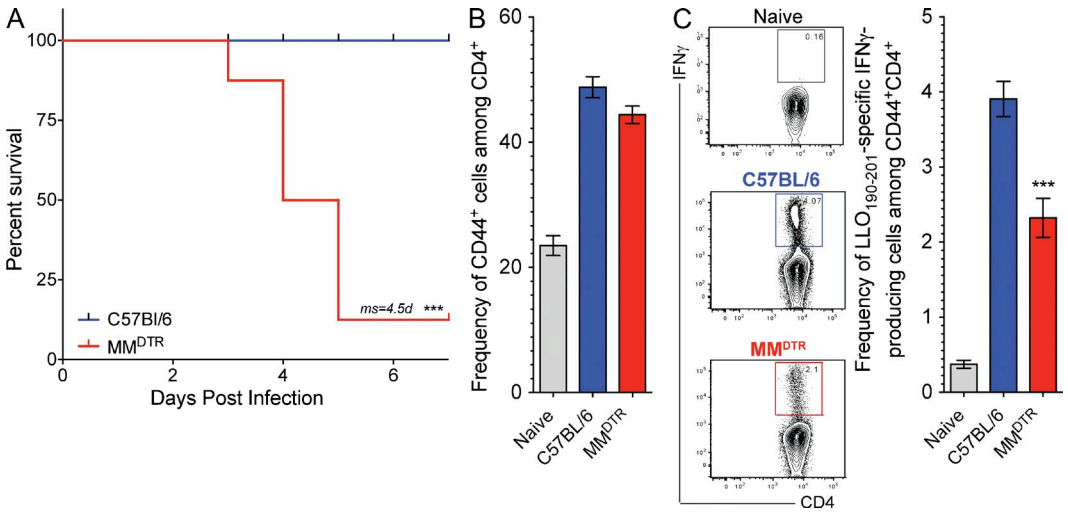

Figure 6. Monocytes and macrophage depletion during *L. monocytogenes* infection. (A–C) C57Bl/6 and MM^{DTR} bone marrow chimeric mice received one DT injection 1 d before i.v. injection with (A) 5 × 10^4 virulent Lm or (B and C) 10^8 ActA Lm and every other day thereafter. Mice were sacrificed at day 7 after infection. (A) Percent of DT-injected C57Bl/6 and MM^{DTR} mice surviving virulent Lm infection. Mean survival (ms) for MM^{DTR} group is 4.5 d. ***, P < 0.000, as compared with B6 control receiving continuous DT. Each group contains eight individual mice. (B) Frequency of CD44$^+$ cells among total spleen CD4$^+$ T cells. No statistical significance among C57Bl/6 and MM^{DTR} groups. (C) Flow cytometry plots from splenocytes isolated 7 d after Lm infection. Cells were stimulated ex vivo with LLO$_{190-201}$ peptide in the presence of BFA, and stained for IFN-γ. Representative plots show Lin^{neg}TCRβ$^+$CD4$^+$CD44$^+$ cells. Bar graph shows frequency of IFN-γ$^+$–producing cells among CD4$^+$CD44$^+$ cells. Data pooled from >3 experiments, 7–11 mice per group. ***, P < 0.001. Error bars indicate SEM.

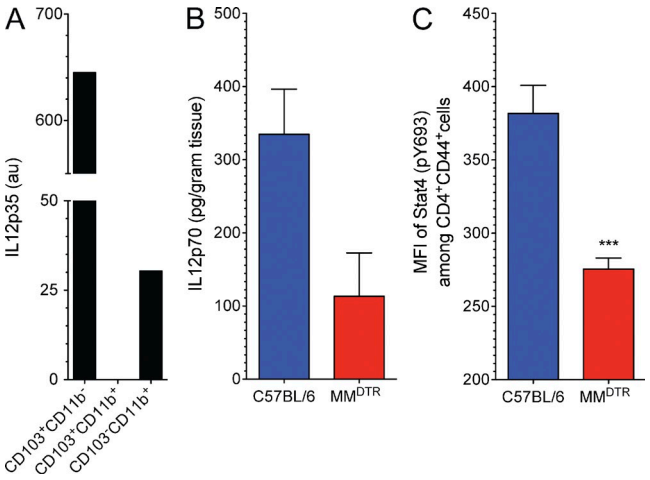

Figure 7. Localized IL-12 reduction after monocyte and macrophage depletion during *C. rodentium* infection. (A) IL12p35 transcript levels from FACS-sorted lamina propria CD103$^+$CD11b$^-$, CD103$^+$CD11b$^+$, and CD103$^-$CD11b$^+$ cells 3 d after *C. rodentium* infection in B6 mice. (B) IL12p70 protein levels in the supernatant of colonic tissue, taken 3 d after *C. rodentium* infection, and cultured for 24 h. (C) Median Fluorescent Intensity (MFI) of Stat4 (pY693) of Lin^{neg}CD45$^+$TCRβ$^+$CD4$^+$CD44^{high} cells. Results represent two experiments with three mice per group per experiment. *, $P < 0.05$; ***, $P < 0.001$. Error bars indicate SEM.

2007). Subsets of monocytes and macrophages can be depleted using clodronate liposomes or antibodies to CSF1R, but neither is specific for these cells (MacDonald et al., 2010; Chow et al., 2011). Genetic deletion of *Csf1r* or *Csf1* also results in loss of monocytes and tissue macrophages, but experiments in these mice are difficult to interpret because of additional severe pleiotropic effects, including infertility, osteoporosis, neural development, low body weight, and severe skeletal abnormalities (Wiktor-Jedrzejczak et al., 1990; Dai et al., 2002). The most frequently used mouse model to study monocyte function is the Ccr2$^{-/-}$ mouse (Boring et al., 1997; Kuziel et al., 1997), wherein monocytes accumulate in the bone marrow due to a defect in migration (Boring et al., 1997; Peters et al., 2004; Serbina and Pamer, 2006; Tsou et al., 2007; Hohl et al., 2009; Nakano et al., 2009). Most importantly, however, CCR2 is also expressed on CD103$^+$ DCs, NK cells, mature T cells, and activated Th1 cells (Kim et al., 2001; Egan et al., 2009; Hohl et al., 2009; Zhang et al., 2010), and therefore the precise role of monocytes in Ccr2$^{-/-}$ and Ccr2^{DTR} mice is difficult to discern with confidence. The *Cx$_3$cr1* gene has also been used to study monocyte and macrophage function, but it is also expressed on NK cells and CD11b$^+$ cells (Jung et al., 2000). *Cx$_3$cr1*$^{-/-}$ mice have been useful because they show impaired trafficking of monocytes and other CX$_3$CR1–expressing cells, but they show normal monocyte development (Auffray et al., 2009). Finally, the combination of conditional expression of DTR under the control of CX$_3$CR1 (CX$_3$CR1$^{LsL\text{-}DTR}$) and CD11c^{cre} leads to selective depletion of CX$_3$CR1^{high} macrophage-like cells in the gut, leaving CX$_3$CR1^{int} cells and monocytes unaffected (Diehl et al., 2013). In contrast, DT injection in MM^{DTR} mice depletes all monocytes and macrophage populations examined, and does not alter cDC or lymphocytes, and therefore, these mice help to clarify the role of monocytes and macrophages in inflammation and immunity.

Comparison of zDC^{DTR} and MM^{DTR} mice allows for analysis of the origins of complex mixtures of mononuclear phagocytes in tissues (Ginhoux et al., 2009; Hashimoto et al., 2011). The intestinal lamina propria contains a particularly diverse group of these cells, all of which express relatively high levels of CD11c and MHCII (Varol et al., 2010; Bogunovic et al., 2012; Tamoutounour et al., 2012). As expected, the CD103$^+$CD11b$^-$ (cDCs) and CD103$^-$CD11b$^+$ (majority monocytes/macrophages) in this mixture were significantly depleted in zDC^{DTR} and MM^{DTR} mice, respectively (Varol et al., 2007, 2009; Bogunovic et al., 2009; Yona et al., 2013). In contrast, the origin of CD103$^+$CD11b$^+$ DCs has been debated. These cells express intermediate levels of F4/80 and Csf1r and show a gene expression signature that does not cluster entirely with either cDCs or macrophages (Uematsu et al., 2008; Bogunovic et al., 2009; Miller et al., 2012). They are deleted in CD11c^{cre} x Notch2$^{fl/fl}$ mice, and they are in part Flt3-dependent for their development, suggesting a preDC origin (Bogunovic et al., 2009; Lewis et al., 2011). However, CD11c and Notch2 are also expressed in some monocytes (Jönsson et al., 2001), and this population is heterogeneous for CD64, further suggesting that a portion are derived from monocytes (Gautier et al., 2012; Langlet et al., 2012; Tamoutounour et al., 2012). Our experiments comparing zDC^{DTR} and MM^{DTR} clarify these apparently contradictory results and reveal that CD103$^+$CD11b$^+$ DCs are a heterogeneous group of cells, some of which originate from preDCs and others from monocytes.

Although CD103$^+$CD11b$^+$ cDCs originating from preDCs cannot be distinguished from their monocytic counterparts by surface marker expression, our results show that the two cell types differ functionally in that only preDC-derived CD103$^+$CD11b$^+$ migrate to the local lymph nodes after *C. rodentium* infection. Antigenic transport, induction of oral tolerance and mucosal immunity require CCR7-dependent migration of CD103$^+$ cells to the mesenteric lymph nodes (Johansson-Lindbom et al., 2005; Worbs et al., 2006; Jaensson et al., 2008; Bogunovic et al., 2009; Cerovic et al., 2013; Diehl et al., 2013; Farache et al., 2013; Schulz et al., 2009; Zigmond et al., 2012). We found that these CD103$^+$ migratory cells predominantly belong to the preDC-derived lineage. Other cells, such as monocyte-derived CD103$^+$CD11b$^+$ and CD103$^-$CD11b$^+$ cells (depleted in lamina propria of DT-treated MM^{DTR}) do not appear to contribute to the transport of *C. rodentium* to the MLNs or the priming of naive T cells. In contrast, Diehl et al. (2013) have described a small subset of CX$_3$CR1^{high} mononuclear phagocytes that appear to migrate after depletion of intestinal microbiota by quadruple antibiotic therapy before infection with a nonpathogenic strain of *Salmonella enterica*. Thus, signals provided by microbiota depletion and noninvasive *S. enterica* infection, but absent during *C. rodentium* or invasive *S. enterica* infection, might mobilize these cells for migration (Diehl et al., 2013;

Farache et al., 2013). In conclusion, zDC^{DTR} and MM^{DTR} mice can be used to distinguish the origins and functions of complex mixtures of mononuclear cells in tissues, despite their phenotypic similarities.

Our experiments are consistent with the work of others showing that cDCs are essential to initiating adaptive T cell immunity in the gut after infection with *C. rodentium* (Hirata et al., 2010). Furthermore, purified lamina propria CD103$^+$ CD11b$^+$ cells promote Th17 T cell differentiation in vitro (Denning et al., 2007, 2011; Denning et al., 2007; Rivollier et al., 2012; Uematsu et al., 2008). Moreover, CD11c^{cre} x Notch2$^{fl/fl}$ mice that lack CD103$^+$CD11b$^+$ cells showed reduced numbers of IL-17–producing Th17 cells (Lewis et al., 2011). Whether this effect was caused by preDC- or monocyte-derived cells could not be determined. Our finding that the IL-17 response is not altered by monocyte and macrophage depletion, but is significantly reduced in zDC^{DTR} mice, suggests that it is the migratory preDC-derived subset within the CD103$^+$CD11b$^+$ population that is necessary for Th17 mucosal immunity.

The role of monocytes and macrophages in the adaptive immune response has been difficult to define, in part because of their ability to produce a variety of cytokines under different physiological and pathological conditions (Gordon and Taylor, 2005). For example, CD103$^-$CD11b$^+$F4/80$^+$ macrophages located in the lamina propria and the serosa normally express IL10 and other antiinflammatory cytokines (Denning et al., 2007; Hadis et al., 2011; Rivollier et al., 2012), but can produce proinflammatory cytokines such as IL-12 in response to infection (Dunay et al., 2008; Kim et al., 2011; Goldszmid et al., 2012; Rivollier et al., 2012). In contrast, cDCs produce far greater amounts of IL-12 and have been shown to be required for Th1 polarization during immune response to *Toxoplasma gondii*, *Listeria monocytogenes*, and *Leishmania donovani* and after TLR ligation (Heufler et al., 1996; Reis e Sousa et al., 1997; Gorak et al., 1998; Maldonado-López et al., 1999; Reinhardt et al., 2006). How monocyte- and macrophage-derived antiinflammatory or proinflammatory cytokines might contribute to adaptive responses in vivo can only be determined by their specific deletion. Our experiments show that despite lower levels of IL-12 production per cell by CD103$^-$ CD11b$^+$ compared with cDCs, the former are essential for intestinal IL-12 production, Stat4 phosphorylation, and an optimal Th1 response to *C. rodentium*.

In conclusion, monocytes and macrophages contribute to adaptive immune responses in the gut and do so by producing cytokines that are essential for optimal Th1 polarization during infection.

MATERIALS AND METHODS

Mice. *Csf1r*$^{LsL\text{-}DTR}$ transgenic mice were generated by DNA microinjection into mouse oocytes. Founder lines were bred to C57BL/6 mice. Three different founder strains were maintained and compared, but no differences were observed. Expression of a DTR-mCherry fusion protein is under the control of the Csf1r gene in *Csf1r*$^{LsL\text{-}DTR}$ mice, but is inhibited by a loxp-flanked Stop element. Expression of Cre recombinase excises the Stop element and allows transcription and translation of DTR-mCherry in cells expressing Csf1r.

zDC^{DTR} mice (Meredith et al., 2012) were bred and housed at The Rockefeller University. C57BL/6, C57BL/6.SJL, and CD11c-DTR mice were purchased from The Jackson Laboratory. Bone marrow chimera recipients were irradiated with 2 doses of 525 rad 3 h apart, and injected with of 5–10 × 10^6 bone marrow cells. Bone marrow chimeras were reconstituted for a minimum of 8 wk after irradiation. All mice were housed in The Rockefeller University Comparative Bioscience Center under specific pathogen–free conditions. All experiments were performed in accordance with the National Institutes of Health guidelines and approved by The Rockefeller University Animal Care and Use Committee.

Infections. For *C. rodentium* infection, mice were orally infected with 2 × 10^9 CFU. Successful infection was confirmed by plating feces and determination of the pathogen burden on day 4 after infection. Weight loss and appearance of infected mice was monitored daily. Mice that lost >20% of their initial body weight or that appeared moribund were sacrificed. Survival experiments were monitored up to day 22 after infection. At this time point, mice had either succumbed to the infection or cleared the infection (as determined by fecal CFU). For *L. monocytogenes* infection, mice were i.v. infected with 5 × 10^4 or 10^8 CFU of virulent or ΔActA mutant *Lm* (S. Way, University of Minnesota, Minneapolis, MN), respectively.

DT injections. DT was purchased from Sigma-Aldrich, and was titrated and tested to determine the lowest effective dose. For transient DT ablation, zDC^{DTR} bone marrow chimeras were injected i.p. with 20 ng DT per gram of body weight (~500 ng per mouse) on the first day of DC depletion and with 4 ng DT per gram body weight (~100 ng per mouse) on all subsequent days. B6, CD11c^{DTR}, and MM^{DTR} bone marrow chimeras received 4 ng DT per gram body weight (~100 ng per mouse) at any time. To analyze cell depletion, mice were euthanized 18–24 h after DT injection. For prolonged cell depletion, DT was injected every 48 h.

Flow cytometry and cell sorting. For FACS analysis, cells were stained using antibodies against F4/80-FITC (BM8), CD103-PE (2E7), CD11c-PerCp-Cy5.5 (M1/70), CD11c-PE-Cy7 (N418), CD115-APC (AFS98), MHCII-eF780 (M5/114.15.2), CD45-eF605NC (30-F110), B220-eF450 (PK136), CD19-eF450 (RA3-6B2), NK1.1-eF450 (eBio1D3), CD11b-eF450 (M1/70), CD44-PE-Cy7 (1M7), and CD4-eF780 (RM4-5; eBioscience), and Ly6C-FITC (AL-21), Ly6G-V450 (1A8), TCRβ-FITC (H57-597), IFN-γ-PE (181157), IL-17A-647 (TC11-18H10), and STAT4-647 (pY693; and BD). DAPI was added to exclude dead cells from analysis. For intracellular cytokine staining, cells were stimulated for 4 h using Leukocyte Activation Cocktail with GolgiPlug (BD). Surface-stained cells were fixed with Cytofix/Cytoperm (BD) and washed with Perm/Wash buffer (BD). Cells were analyzed on a LSR Fortessa flow cytometer (BD). Analysis was performed using FlowJo software (Tree Star). Cell sorting was performed on a FACSAriaIII cell sorter (BD). Prism 4 (GraphPad Software) was used for statistical analyses.

Spleen and LN cell isolation. Spleen and lymph nodes were isolated, mechanically disrupted, and incubated with HBSS + 5% FBS + 0.5 mg/ml Collagenase (Roche) at 37°C for 30 min. Cells were filtered through 100-μM cell strainers and washed. For spleen cells, erythrocytes were lysed with ACK Lysing buffer (Gibco). Cells were counted, and up to 10^6 cells were stained for FACS analysis.

Intestinal cell isolation. Small bowel (jejunum and ileum) and large bowel (cecum and colon) were carefully excised, and mesentery and fat were removed. Feces were removed, and Peyer's patches were excised from the small intestine. Both small and large bowel were opened longitudinally and rinsed in HBSS (Gibco), followed by HBSS + 1 mM DTT (Sigma-Aldrich). Small and large bowel were cut into 1-cm pieces and incubated with 25 ml of HBSS + 5% FBS + 5 mM EDTA for 15 min at 37°C at 230 rpm. Tubes were briefly vortexed, and supernatant containing intraepithelial lymphocytes was decanted. Bowel was washed with 10 ml of HBSS + 5% FBS for 15 min at 37°C at 230 rpm. The gut tissues were then finely chopped and digested in

HBSS + 5% FBS + 1X sodium pyruvate + 25 mM Hepes + 50 µg/ml DNaseI + 0.05 mg/ml Collagenase VIII for 1 h at 37°C at 100 rpm. After passing the tissue through a 100-µm cell strainer, cells were separated by discontinuous Percoll gradient (70%/35%) centrifugation. Mononuclear cells were isolated from the interphase, washed, and either stained for FACS analysis or restimulated with Leukocyte Activation Cocktail with GolgiPlug (BD).

For separate isolation of lamina propria cells from the serosa/muscularis, Peyer's patches were removed and bowels were cut open and washed three times with HBSS + 5% FBS. Bowels were then incubated with HBSS + 1 mM DTT for 20 min at 37°C at 230 rpm and subsequently washed with HBSS to remove DTT. Gut tissues were incubated with PBS + 1.3 mM EDTA for 60 min at 37°C at 230 rpm. After that, the serosa/muscularis was separated from the lamina propria using dissection microscope. The separated tissues were processed as described above. The tissue was then homogenized with an 18-gauge needle and filtered through a 70-µm cell strainer.

Isolation of tissue macrophages. Peritoneal macrophages were isolated from peritoneal lavages. Lungs and livers were isolated after perfusion of sacrificed mice. Tissue was cut into small pieces and incubated with HBSS + 5% FBS + 0.5 mg/ml Collagenase + 50 µg/ml DNaseI at 37°C for 60 min. After passing the tissue through a 100 µm cell strainer, cells were separated by discontinuous Percoll gradient (70%/35%) centrifugation. Mononuclear cells were isolated from the interphase.

Fluorescent microscopy. Tissues were fixed in 3% PFA and 25% sucrose overnight, frozen in O.C.T Compound (Tissue-Tek; Sakura) and stored at −80°C. Frozen tissue was cut into 20-µm thick sections, fixed for 10 min in ice-cold acetone, and rehydrated in PBS for 30 min. Tissue sections were outlined with a Pap pen and stained for 2 h at room temperature in 1% FCS in PBS. Antibody cocktail contained anti-CD16/CD32 blocking Ab (2.4G2, 1:100; BD), FITC anti-CD45R/B220 (RA3-6B2, 1:200; BD), and one of the following: APC anti-F4/80 (BM8, 1:100; eBioscience), Alexa Fluor 647 anti-CD209b/SIGN-R1 (eBio22D1, 1:100; eBioscience), and Alexa Fluor 647 anti-CD169 (MOMA-1, 1:100; AbD Serotec). Sections were washed for 10 min 3× and mounted using ProLong Gold Antifade Reagent with DAPI (Invitrogen). Images were acquired on a wide-field fluorescent microscope (Carl Zeiss) using MetaVue acquisition software (Molecular Devices) and an Orca ER B/W digital camera (Hamamatsu) at The Rockefeller University Bio-Imaging Resource Center.

Organ culture. To determine IL-12 levels in the intestines, weighed explants were cultured for 24 h in complete RPMI in the presence of penicillin, streptomycin, and gentamycin. Centrifuged supernatant was frozen down and used for ELISA.

ELISA. Serum levels of MCSF, GMCSF, and Flt3L were determined by ELISA using the respective Quantikine immunoassay (R&D Systems) according to the manufacturer's protocol. Il12p70 levels were determined in the supernatant of explant cultures with an IL12p70-specific ELISA (eBioscience) according to the manufacturer's protocol.

qRT-PCR. Total RNA was isolated from FACS-sorted single-cell suspensions with TRIzol (Invitrogen), from which cDNA libraries were reverse transcribed using Superscript II (Invitrogen) and random primers. Total RNA from tissue was isolated with the Direct-zol RNA MiniPrep kit (Zymo Research) and cDNA libraries were generated as described above. GAPDH forward: 5′-TGAAGCAGGCATCTGAGGG-3′, GAPDH reverse: 5′-CGAAGGTGGAAGAGTGGGAG-3′, IL12p35 forward: 5′-CTGTGCCTTGGTAGCATCTATG-3′, IL12p35 reverse: 5′-GCAGAGTCTCGCCATTATGATTC-3′, Ccr7 forward: 5′-TGTACGAGTCGGTGTGCTTC-3′, Ccr7 reverse: 5′-GGTAGGTATCCGTCATGGTCTTG-3′.

All quantitative PCR reactions were performed with Brilliant SYBR Green (Agilent Technologies) on an Mx3005P system (Agilent Technologies).

T cell priming. 5×10^6 violet trace–labeled OT-II cells were transferred in DT-injected B6, zDC^{DTR}, and MM^{DTR} mice. The next day mice were infected with 2×10^9 CFU of a *C. rodentium* strain that was transformed with a plasmid encoding Ovalbumin. 1 g/liter of Kanamycin was added to the drinking water to ensure the expression of Ovalbumin. Mice were again injected with DT 1 and 3 d after the infection. T cell proliferation and activation in the mesenteric LN was determined 5 d after the infection.

Statistical Analysis. Results are given as a mean ± SE or mean ± SD. Comparisons between groups were done using two-tailed Student's *t* test analysis. Survival curve comparison was performed using a log-ranked Mantel-Cox test. Statistical significance was determined as p-values less than 0.05.

We are grateful to members of the Nussenzweig laboratory for helpful discussion, reagents, or critical reading of the manuscript. We would like to thank K. Velinzon and L. Shatalina for cell sorting. We express specials thanks to Dr. Singsing Way (University of Minnesota, MN) for his gift of the ΔActA *L. monocytogenes* strain.

This work was supported in part by National Institutes of Health (NIH) grant number AI051573. M.C. Nussenzweig is an Howard Hughes Medical Insitute investigator. H.A. Schreiber was supported by a NIH Ruth L. Kirschstein Individual Postdoctoral Fellowship F32 AI096721. J. Loschko was supported by Deutsche Forschungsgemeinschaft DFG LO1864/1.

The authors report no competing financial interests.

Submitted: 1 May 2013
Accepted: 8 August 2013

REFERENCES

Athie-Morales, V., H.H. Smits, D.A. Cantrell, and C.M. Hilkens. 2004. Sustained IL-12 signaling is required for Th1 development. *J. Immunol.* 172:61–69.

Auffray, C., D.K. Fogg, E. Narni-Mancinelli, B. Senechal, C. Trouillet, N. Saederup, J. Leemput, K. Bigot, L. Campisi, M. Abitbol, et al. 2009. $CX3CR1^+$ $CD115^+$ $CD135^+$ common macrophage/DC precursors and the role of CX3CR1 in their response to inflammation. *J. Exp. Med.* 206:595–606. http://dx.doi.org/10.1084/jem.20081385

Basu, R., D.B. O'Quinn, D.J. Silberger, T.R. Schoeb, L. Fouser, W. Ouyang, R.D. Hatton, and C.T. Weaver. 2012. Th22 cells are an important source of IL-22 for host protection against enteropathogenic bacteria. *Immunity.* 37:1061–1075. http://dx.doi.org/10.1016/j.immuni.2012.08.024

Bennett, C.L., and B.E. Clausen. 2007. DC ablation in mice: promises, pitfalls, and challenges. *Trends Immunol.* 28:525–531. http://dx.doi.org/10.1016/j.it.2007.08.011

Bogunovic, M., F. Ginhoux, J. Helft, L. Shang, D. Hashimoto, M. Greter, K. Liu, C. Jakubzick, M.A. Ingersoll, M. Leboeuf, et al. 2009. Origin of the lamina propria dendritic cell network. *Immunity.* 31:513–525. http://dx.doi.org/10.1016/j.immuni.2009.08.010

Bogunovic, M., A. Mortha, P.A. Muller, and M. Merad. 2012. Mononuclear phagocyte diversity in the intestine. *Immunol. Res.* 54:37–49. http://dx.doi.org/10.1007/s12026-012-8323-5

Boring, L., J. Gosling, S.W. Chensue, S.L. Kunkel, R.V. Farese Jr., H.E. Broxmeyer, and I.F. Charo. 1997. Impaired monocyte migration and reduced type 1 (Th1) cytokine responses in C-C chemokine receptor 2 knockout mice. *J. Clin. Invest.* 100:2552–2561. http://dx.doi.org/10.1172/JCI119798

Bry, L., and M.B. Brenner. 2004. Critical role of T cell-dependent serum antibody, but not the gut-associated lymphoid tissue, for surviving acute mucosal infection with *Citrobacter rodentium*, an attaching and effacing pathogen. *J. Immunol.* 172:433–441.

Bry, L., M. Brigl, and M.B. Brenner. 2006. CD4+-T-cell effector functions and costimulatory requirements essential for surviving mucosal infection with *Citrobacter rodentium*. *Infect. Immun.* 74:673–681. http://dx.doi.org/10.1128/IAI.74.1.673-681.2006

Cerovic, V., S.A. Houston, C.L. Scott, A. Aumeunier, U. Yrlid, A.M. Mowat, and S.W. Milling. 2013. Intestinal CD103(-) dendritic cells migrate in lymph and prime effector T cells. *Mucosal Immunol.* 6:104–113. http://dx.doi.org/10.1038/mi.2012.53

Chow, A., B.D. Brown, and M. Merad. 2011. Studying the mononuclear phagocyte system in the molecular age. *Nat. Rev. Immunol.* 11:788–798. http://dx.doi.org/10.1038/nri3087

Clausen, B.E., C. Burkhardt, W. Reith, R. Renkawitz, and I. Förster. 1999. Conditional gene targeting in macrophages and granulocytes using LysMcre mice. *Transgenic Res.* 8:265–277. http://dx.doi.org/10.1023/A:1008942828960

Dai, X.M., G.R. Ryan, A.J. Hapel, M.G. Dominguez, R.G. Russell, S. Kapp, V. Sylvestre, and E.R. Stanley. 2002. Targeted disruption of the mouse colony-stimulating factor 1 receptor gene results in osteopetrosis, mononuclear phagocyte deficiency, increased primitive progenitor cell frequencies, and reproductive defects. *Blood.* 99:111–120. http://dx.doi.org/10.1182/blood.V99.1.111

Denning, T.L., Y.C. Wang, S.R. Patel, I.R. Williams, and B. Pulendran. 2007. Lamina propria macrophages and dendritic cells differentially induce regulatory and interleukin 17-producing T cell responses. *Nat. Immunol.* 8:1086–1094. http://dx.doi.org/10.1038/ni1511

Denning, T.L., B.A. Norris, O. Medina-Contreras, S. Manicassamy, D. Geem, R. Madan, C.L. Karp, and B. Pulendran. 2011. Functional specializations of intestinal dendritic cell and macrophage subsets that control Th17 and regulatory T cell responses are dependent on the T cell/APC ratio, source of mouse strain, and regional localization. *J. Immunol.* 187:733–747. http://dx.doi.org/10.4049/jimmunol.1002701

Diehl, G.E., R.S. Longman, J.X. Zhang, B. Breart, C. Galan, A. Cuesta, S.R. Schwab, and D.R. Littman. 2013. Microbiota restricts trafficking of bacteria to mesenteric lymph nodes by CX(3)CR1(hi) cells. *Nature.* 494:116–120. http://dx.doi.org/10.1038/nature11809

Dunay, I.R., R.A. Damatta, B. Fux, R. Presti, S. Greco, M. Colonna, and L.D. Sibley. 2008. Gr1(+) inflammatory monocytes are required for mucosal resistance to the pathogen Toxoplasma gondii. *Immunity.* 29:306–317. http://dx.doi.org/10.1016/j.immuni.2008.05.019

Egan, C.E., M.D. Craven, J. Leng, M. Mack, K.W. Simpson, and E.Y. Denkers. 2009. CCR2-dependent intraepithelial lymphocytes mediate inflammatory gut pathology during Toxoplasma gondii infection. *Mucosal Immunol.* 2:527–535. http://dx.doi.org/10.1038/mi.2009.105

Farache, J., I. Koren, I. Milo, I. Gurevich, K.W. Kim, E. Zigmond, G.C. Furtado, S.A. Lira, and G. Shakhar. 2013. Luminal bacteria recruit CD103(+) dendritic cells into the intestinal epithelium to sample bacterial antigens for presentation. *Immunity.* 38:581–595.

Fogg, D.K., C. Sibon, C. Miled, S. Jung, P. Aucouturier, D.R. Littman, A. Cumano, and F. Geissmann. 2006. A clonogenic bone marrow progenitor specific for macrophages and dendritic cells. *Science.* 311:83–87. http://dx.doi.org/10.1126/science.1117729

Gautier, E.L., T. Shay, J. Miller, M. Greter, C. Jakubzick, S. Ivanov, J. Helft, A. Chow, K.G. Elpek, S. Gordonov, et al; Immunological Genome Consortium. 2012. Gene-expression profiles and transcriptional regulatory pathways that underlie the identity and diversity of mouse tissue macrophages. *Nat. Immunol.* 13:1118–1128. http://dx.doi.org/10.1038/ni.2419

Geissmann, F., C. Auffray, R. Palframan, C. Wirrig, A. Ciocca, L. Campisi, E. Narni-Mancinelli, and G. Lauvau. 2008. Blood monocytes: distinct subsets, how they relate to dendritic cells, and their possible roles in the regulation of T-cell responses. *Immunol. Cell Biol.* 86:398–408. http://dx.doi.org/10.1038/icb.2008.19

Geissmann, F., S. Gordon, D.A. Hume, A.M. Mowat, and G.J. Randolph. 2010a. Unravelling mononuclear phagocyte heterogeneity. *Nat. Rev. Immunol.* 10:453–460. http://dx.doi.org/10.1038/nri2784

Geissmann, F., M.G. Manz, S. Jung, M.H. Sieweke, M. Merad, and K. Ley. 2010b. Development of monocytes, macrophages, and dendritic cells. *Science.* 327:656–661. http://dx.doi.org/10.1126/science.1178331

Ginhoux, F., K. Liu, J. Helft, M. Bogunovic, M. Greter, D. Hashimoto, J. Price, N. Yin, J. Bromberg, S.A. Lira, et al. 2009. The origin and development of nonlymphoid tissue CD103+ DCs. *J. Exp. Med.* 206:3115–3130. http://dx.doi.org/10.1084/jem.20091756

Goldszmid, R.S., P. Caspar, A. Rivollier, S. White, A. Dzutsev, S. Hieny, B. Kelsall, G. Trinchieri, and A. Sher. 2012. NK cell-derived interferon-γ orchestrates cellular dynamics and the differentiation of monocytes into dendritic cells at the site of infection. *Immunity.* 36:1047–1059. http://dx.doi.org/10.1016/j.immuni.2012.03.026

Gorak, P.M., C.R. Engwerda, and P.M. Kaye. 1998. Dendritic cells, but not macrophages, produce IL-12 immediately following *Leishmania donovani* infection. *Eur. J. Immunol.* 28:687–695. http://dx.doi.org/10.1002/(SICI)1521-4141(199802)28:023.0.CO;2-N

Gordon, S., and P.R. Taylor. 2005. Monocyte and macrophage heterogeneity. *Nat. Rev. Immunol.* 5:953–964. http://dx.doi.org/10.1038/nri1733

Hadis, U., B. Wahl, O. Schulz, M. Hardtke-Wolenski, A. Schippers, N. Wagner, W. Müller, T. Sparwasser, R. Förster, and O. Pabst. 2011. Intestinal tolerance requires gut homing and expansion of FoxP3+ regulatory T cells in the lamina propria. *Immunity.* 34:237–246. http://dx.doi.org/10.1016/j.immuni.2011.01.016

Hashimoto, D., J. Miller, and M. Merad. 2011. Dendritic cell and macrophage heterogeneity in vivo. *Immunity.* 35:323–335. http://dx.doi.org/10.1016/j.immuni.2011.09.007

Heufler, C., F. Koch, U. Stanzl, G. Topar, M. Wysocka, G. Trinchieri, A. Enk, R.M. Steinman, N. Romani, and G. Schuler. 1996. Interleukin-12 is produced by dendritic cells and mediates T helper 1 development as well as interferon-gamma production by T helper 1 cells. *Eur. J. Immunol.* 26:659–668. http://dx.doi.org/10.1002/eji.1830260323

Higgins, L.M., G. Frankel, G. Douce, G. Dougan, and T.T. MacDonald. 1999. *Citrobacter rodentium* infection in mice elicits a mucosal Th1 cytokine response and lesions similar to those in murine inflammatory bowel disease. *Infect. Immun.* 67:3031–3039.

Hirata, Y., L. Egea, S.M. Dann, L. Eckmann, and M.F. Kagnoff. 2010. GM-CSF-facilitated dendritic cell recruitment and survival govern the intestinal mucosal response to a mouse enteric bacterial pathogen. *Cell Host Microbe.* 7:151–163. http://dx.doi.org/10.1016/j.chom.2010.01.006

Hohl, T.M., A. Rivera, L. Lipuma, A. Gallegos, C. Shi, M. Mack, and E.G. Pamer. 2009. Inflammatory monocytes facilitate adaptive CD4 T cell responses during respiratory fungal infection. *Cell Host Microbe.* 6:470–481. http://dx.doi.org/10.1016/j.chom.2009.10.007

Hsieh, C.S., S.E. Macatonia, C.S. Tripp, S.F. Wolf, A. O'Garra, and K.M. Murphy. 1993. Development of TH1 CD4+ T cells through IL-12 produced by Listeria-induced macrophages. *Science.* 260:547–549. http://dx.doi.org/10.1126/science.8097338

Jaensson, E., H. Uronen-Hansson, O. Pabst, B. Eksteen, J. Tian, J.L. Coombes, P.L. Berg, T. Davidsson, F. Powrie, B. Johansson-Lindbom, and W.W. Agace. 2008. Small intestinal $CD103^+$ dendritic cells display unique functional properties that are conserved between mice and humans. *J. Exp. Med.* 205:2139–2149. http://dx.doi.org/10.1084/jem.20080414

Johansson-Lindbom, B., M. Svensson, O. Pabst, C. Palmqvist, G. Marquez, R. Förster, and W.W. Agace. 2005. Functional specialization of gut CD103+ dendritic cells in the regulation of tissue-selective T cell homing. *J. Exp. Med.* 202:1063–1073. http://dx.doi.org/10.1084/jem.20051100

Jönsson, J.I., Z. Xiang, M. Pettersson, M. Lardelli, and G. Nilsson. 2001. Distinct and regulated expression of Notch receptors in hematopoietic lineages and during myeloid differentiation. *Eur. J. Immunol.* 31:3240–3247. http://dx.doi.org/10.1002/1521-4141(200111)31:113.0.CO;2-E

Jung, S., J. Aliberti, P. Graemmel, M.J. Sunshine, G.W. Kreutzberg, A. Sher, and D.R. Littman. 2000. Analysis of fractalkine receptor CX(3)CR1 function by targeted deletion and green fluorescent protein reporter gene insertion. *Mol. Cell. Biol.* 20:4106–4114. http://dx.doi.org/10.1128/MCB.20.11.4106-4114.2000

Jung, S., D. Unutmaz, P. Wong, G. Sano, K. De los Santos, T. Sparwasser, S. Wu, S. Vuthoori, K. Ko, F. Zavala, et al. 2002. In vivo depletion of CD11c+ dendritic cells abrogates priming of CD8+ T cells by exogenous cell-associated antigens. *Immunity.* 17:211–220. http://dx.doi.org/10.1016/S1074-7613(02)00365-5

Kim, C.H., L. Rott, E.J. Kunkel, M.C. Genovese, D.P. Andrew, L. Wu, and E.C. Butcher. 2001. Rules of chemokine receptor association with T cell polarization in vivo. *J. Clin. Invest.* 108:1331–1339.

Kim, Y.G., N. Kamada, M.H. Shaw, N. Warner, G.Y. Chen, L. Franchi, and G. Núñez. 2011. The Nod2 sensor promotes intestinal pathogen eradication via the chemokine CCL2-dependent recruitment of inflammatory monocytes. *Immunity.* 34:769–780. http://dx.doi.org/10.1016/j.immuni.2011.04.013

Kuziel, W.A., S.J. Morgan, T.C. Dawson, S. Griffin, O. Smithies, K. Ley, and N. Maeda. 1997. Severe reduction in leukocyte adhesion and monocyte extravasation in mice deficient in CC chemokine receptor 2. *Proc. Natl. Acad. Sci. USA.* 94:12053–12058. http://dx.doi.org/10.1073/pnas.94.22.12053

Langlet, C., S. Tamoutounour, S. Henri, H. Luche, L. Ardouin, C. Grégoire, B. Malissen, and M. Guilliams. 2012. CD64 expression distinguishes monocyte-derived and conventional dendritic cells and reveals their distinct role during intramuscular immunization. *J. Immunol.* 188:1751–1760. http://dx.doi.org/10.4049/jimmunol.1102744

Lee, S.H., P.M. Starkey, and S. Gordon. 1985. Quantitative analysis of total macrophage content in adult mouse tissues. Immunochemical studies with monoclonal antibody F4/80. *J. Exp. Med.* 161:475–489. http://dx.doi.org/10.1084/jem.161.3.475

León, B., M. López-Bravo, and C. Ardavín. 2007. Monocyte-derived dendritic cells formed at the infection site control the induction of protective T helper 1 responses against *Leishmania*. *Immunity*. 26:519–531. http://dx.doi.org/10.1016/j.immuni.2007.01.017

Lewis, K.L., M.L. Caton, M. Bogunovic, M. Greter, L.T. Grajkowska, D. Ng, A. Klinakis, I.F. Charo, S. Jung, J.L. Gommerman, et al. 2011. Notch2 receptor signaling controls functional differentiation of dendritic cells in the spleen and intestine. *Immunity*. 35:780–791. http://dx.doi.org/10.1016/j.immuni.2011.08.013

Liu, K., and M.C. Nussenzweig. 2010. Origin and development of dendritic cells. *Immunol. Rev.* 234:45–54. http://dx.doi.org/10.1111/j.0105-2896.2009.00879.x

Liu, K., G.D. Victora, T.A. Schwickert, P. Guermonprez, M.M. Meredith, K. Yao, F.F. Chu, G.J. Randolph, A.Y. Rudensky, and M. Nussenzweig. 2009. In vivo analysis of dendritic cell development and homeostasis. *Science*. 324:392–397. http://dx.doi.org/10.1126/science.1171243

MacDonald, K.P., J.S. Palmer, S. Cronau, E. Seppanen, S. Olver, N.C. Raffelt, R. Kuns, A.R. Pettit, A. Clouston, B. Wainwright, et al. 2010. An antibody against the colony-stimulating factor 1 receptor depletes the resident subset of monocytes and tissue- and tumor-associated macrophages but does not inhibit inflammation. *Blood*. 116:3955–3963. http://dx.doi.org/10.1182/blood-2010-02-266296

Maldonado-López, R., T. De Smedt, P. Michel, J. Godfroid, B. Pajak, C. Heirman, K. Thielemans, O. Leo, J. Urbain, and M. Moser. 1999. CD8α^+ and CD8α^- subclasses of dendritic cells direct the development of distinct T helper cells in vivo. *J. Exp. Med.* 189:587–592. http://dx.doi.org/10.1084/jem.189.3.587

Mangan, P.R., L.E. Harrington, D.B. O'Quinn, W.S. Helms, D.C. Bullard, C.O. Elson, R.D. Hatton, S.M. Wahl, T.R. Schoeb, and C.T. Weaver. 2006. Transforming growth factor-beta induces development of the T(H)17 lineage. *Nature*. 441:231–234. http://dx.doi.org/10.1038/nature04754

McKenna, H.J., K.L. Stocking, R.E. Miller, K. Brasel, T. De Smedt, E. Maraskovsky, C.R. Maliszewski, D.H. Lynch, J. Smith, B. Pulendran, et al. 2000. Mice lacking flt3 ligand have deficient hematopoiesis affecting hematopoietic progenitor cells, dendritic cells, and natural killer cells. *Blood*. 95:3489–3497.

Meredith, M.M., K. Liu, G. Darrasse-Jeze, A.O. Kamphorst, H.A. Schreiber, P. Guermonprez, J. Idoyaga, C. Cheong, K.H. Yao, R.E. Niec, and M.C. Nussenzweig. 2012. Expression of the zinc finger transcription factor zDC (Zbtb46, Btbd4) defines the classical dendritic cell lineage. *J. Exp. Med.* 209:1153–1165. http://dx.doi.org/10.1084/jem.20112675

Miller, J.C., B.D. Brown, T. Shay, E.L. Gautier, V. Jojic, A. Cohain, G. Pandey, M. Leboeuf, K.G. Elpek, J. Helft, et al; Immunological Genome Consortium. 2012. Deciphering the transcriptional network of the dendritic cell lineage. *Nat. Immunol.* 13:888–899. http://dx.doi.org/10.1038/ni.2370

Mundy, R., T.T. MacDonald, G. Dougan, G. Frankel, and S. Wiles. 2005. *Citrobacter rodentium* of mice and man. *Cell. Microbiol.* 7:1697–1706. http://dx.doi.org/10.1111/j.1462-5822.2005.00625.x

Murphy, K.M., W. Ouyang, J.D. Farrar, J. Yang, S. Ranganath, H. Asnagli, M. Afkarian, and T.L. Murphy. 2000. Signaling and transcription in T helper development. *Annu. Rev. Immunol.* 18:451–494. http://dx.doi.org/10.1146/annurev.immunol.18.1.451

Nakano, H., K.L. Lin, M. Yanagita, C. Charbonneau, D.N. Cook, T. Kakiuchi, and M.D. Gunn. 2009. Blood-derived inflammatory dendritic cells in lymph nodes stimulate acute T helper type 1 immune responses. *Nat. Immunol.* 10:394–402. http://dx.doi.org/10.1038/ni.1707

Ota, N., K. Wong, P.A. Valdez, Y. Zheng, N.K. Crellin, L. Diehl, and W. Ouyang. 2011. IL-22 bridges the lymphotoxin pathway with the maintenance of colonic lymphoid structures during infection with Citrobacter rodentium. *Nat. Immunol.* 12:941–948. http://dx.doi.org/10.1038/ni.2089

Peters, W., J.G. Cyster, M. Mack, D. Schlöndorff, A.J. Wolf, J.D. Ernst, and I.F. Charo. 2004. CCR2-dependent trafficking of F4/80dim macrophages and CD11cdim/intermediate dendritic cells is crucial for T cell recruitment to lungs infected with Mycobacterium tuberculosis. *J. Immunol.* 172:7647–7653.

Reinhardt, R.L., S. Hong, S.J. Kang, Z.E. Wang, and R.M. Locksley. 2006. Visualization of IL-12/23p40 in vivo reveals immunostimulatory dendritic cell migrants that promote Th1 differentiation. *J. Immunol.* 177:1618–1627.

Reis e Sousa, C., S. Hieny, T. Scharton-Kersten, D. Jankovic, H. Charest, R.N. Germain, and A. Sher. 1997. In vivo microbial stimulation induces rapid CD40 ligand-independent production of interleukin 12 by dendritic cells and their redistribution to T cell areas. *J. Exp. Med.* 186:1819–1829. http://dx.doi.org/10.1084/jem.186.11.1819

Rivollier, A., J. He, A. Kole, V. Valatas, and B.L. Kelsall. 2012. Inflammation switches the differentiation program of Ly6Chi monocytes from antiinflammatory macrophages to inflammatory dendritic cells in the colon. *J. Exp. Med.* 209:139–155. http://dx.doi.org/10.1084/jem.20101387

Satoh-Takayama, N., C.A. Vosshenrich, S. Lesjean-Pottier, S. Sawa, M. Lochner, F. Rattis, J.J. Mention, K. Thiam, N. Cerf-Bensussan, O. Mandelboim, et al. 2008. Microbial flora drives interleukin 22 production in intestinal NKp46+ cells that provide innate mucosal immune defense. *Immunity*. 29:958–970. http://dx.doi.org/10.1016/j.immuni.2008.11.001

Schulz, O., E. Jaensson, E.K. Persson, X. Liu, T. Worbs, W.W. Agace, and O. Pabst. 2009. Intestinal CD103+, but not CX3CR1+, antigen sampling cells migrate in lymph and serve classical dendritic cell functions. *J. Exp. Med.* 206:3101–3114. http://dx.doi.org/10.1084/jem.20091925

Schulz, C., E. Gomez Perdiguero, L. Chorro, H. Szabo-Rogers, N. Cagnard, K. Kierdorf, M. Prinz, B. Wu, S.E. Jacobsen, J.W. Pollard, et al. 2012. A lineage of myeloid cells independent of Myb and hematopoietic stem cells. *Science*. 336:86–90. http://dx.doi.org/10.1126/science.1219179

Serbina, N.V., and E.G. Pamer. 2006. Monocyte emigration from bone marrow during bacterial infection requires signals mediated by chemokine receptor CCR2. *Nat. Immunol.* 7:311–317. http://dx.doi.org/10.1038/ni1309

Serbina, N.V., T.P. Salazar-Mather, C.A. Biron, W.A. Kuziel, and E.G. Pamer. 2003. TNF/iNOS-producing dendritic cells mediate innate immune defense against bacterial infection. *Immunity*. 19:59–70. http://dx.doi.org/10.1016/S1074-7613(03)00171-7

Serbina, N.V., T. Jia, T.M. Hohl, and E.G. Pamer. 2008. Monocyte-mediated defense against microbial pathogens. *Annu. Rev. Immunol.* 26:421–452. http://dx.doi.org/10.1146/annurev.immunol.26.021607.090326

Shortman, K., and S.H. Naik. 2007. Steady-state and inflammatory dendritic-cell development. *Nat. Rev. Immunol.* 7:19–30. http://dx.doi.org/10.1038/nri1996

Simmons, C.P., N.S. Goncalves, M. Ghaem-Maghami, M. Bajaj-Elliott, S. Clare, B. Neves, G. Frankel, G. Dougan, and T.T. MacDonald. 2002. Impaired resistance and enhanced pathology during infection with a noninvasive, attaching-effacing enteric bacterial pathogen, *Citrobacter rodentium*, in mice lacking IL-12 or IFN-γ. *J. Immunol.* 168:1804–1812.

Sonnenberg, G.F., L.A. Monticelli, M.M. Elloso, L.A. Fouser, and D. Artis. 2011. CD4(+) lymphoid tissue-inducer cells promote innate immunity in the gut. *Immunity*. 34:122–134. http://dx.doi.org/10.1016/j.immuni.2010.12.009

Steinman, R.M., D. Hawiger, and M.C. Nussenzweig. 2003. Tolerogenic dendritic cells. *Annu. Rev. Immunol.* 21:685–711. http://dx.doi.org/10.1146/annurev.immunol.21.120601.141040

Tamoutounour, S., S. Henri, H. Lelouard, B. de Bovis, C. de Haar, C.J. van der Woude, A.M. Woltman, Y. Reyal, D. Bonnet, D. Sichien, et al. 2012. CD64 distinguishes macrophages from dendritic cells in the gut and reveals the Th1-inducing role of mesenteric lymph node macrophages during colitis. *Eur. J. Immunol.* 42:3150–3166. http://dx.doi.org/10.1002/eji.201242847

Tsou, C.L., W. Peters, Y. Si, S. Slaymaker, A.M. Aslanian, S.P. Weisberg, M. Mack, and I.F. Charo. 2007. Critical roles for CCR2 and MCP-3 in monocyte mobilization from bone marrow and recruitment to inflammatory sites. *J. Clin. Invest.* 117:902–909. http://dx.doi.org/10.1172/JCI29919

Tumanov, A.V., E.P. Koroleva, X. Guo, Y. Wang, A. Kruglov, S. Nedospasov, and Y.X. Fu. 2011. Lymphotoxin controls the IL-22 protection pathway in gut innate lymphoid cells during mucosal pathogen challenge. *Cell Host Microbe*. 10:44–53. http://dx.doi.org/10.1016/j.chom.2011.06.002

Uematsu, S., K. Fujimoto, M.H. Jang, B.G. Yang, Y.J. Jung, M. Nishiyama, S. Sato, T. Tsujimura, M. Yamamoto, Y. Yokota, et al. 2008. Regulation of humoral and cellular gut immunity by lamina propria dendritic cells expressing Toll-like receptor 5. *Nat. Immunol.* 9:769–776. http://dx.doi.org/10.1038/ni.1622

Varol, C., L. Landsman, D.K. Fogg, L. Greenshtein, B. Gildor, R. Margalit, V. Kalchenko, F. Geissmann, and S. Jung. 2007. Monocytes give rise to mucosal, but not splenic, conventional dendritic cells. *J. Exp. Med.* 204:171–180. http://dx.doi.org/10.1084/jem.20061011

Varol, C., A. Vallon-Eberhard, E. Elinav, T. Aychek, Y. Shapira, H. Luche, H.J. Fehling, W.D. Hardt, G. Shakhar, and S. Jung. 2009. Intestinal lamina propria dendritic cell subsets have different origin and functions. *Immunity*. 31:502–512. http://dx.doi.org/10.1016/j.immuni.2009.06.025

Varol, C., E. Zigmond, and S. Jung. 2010. Securing the immune tightrope: mononuclear phagocytes in the intestinal lamina propria. *Nat. Rev. Immunol.* 10:415–426. http://dx.doi.org/10.1038/nri2778

Waskow, C., K. Liu, G. Darrasse-Jèze, P. Guermonprez, F. Ginhoux, M. Merad, T. Shengelia, K. Yao, and M. Nussenzweig. 2008. The receptor tyrosine kinase Flt3 is required for dendritic cell development in peripheral lymphoid tissues. *Nat. Immunol.* 9:676–683. http://dx.doi.org/10.1038/ni.1615

Wiktor-Jedrzejczak, W., A. Bartocci, A.W. Ferrante Jr., A. Ahmed-Ansari, K.W. Sell, J.W. Pollard, and E.R. Stanley. 1990. Total absence of colony-stimulating factor 1 in the macrophage-deficient osteopetrotic (op/op) mouse. *Proc. Natl. Acad. Sci. USA*. 87:4828–4832. http://dx.doi.org/10.1073/pnas.87.12.4828

Witmer-Pack, M.D., D.A. Hughes, G. Schuler, L. Lawson, A. McWilliam, K. Inaba, R.M. Steinman, and S. Gordon. 1993. Identification of macrophages and dendritic cells in the osteopetrotic (op/op) mouse. *J. Cell Sci.* 104:1021–1029.

Worbs, T., U. Bode, S. Yan, M.W. Hoffmann, G. Hintzen, G. Bernhardt, R. Förster, and O. Pabst. 2006. Oral tolerance originates in the intestinal immune system and relies on antigen carriage by dendritic cells. *J. Exp. Med.* 203:519–527. http://dx.doi.org/10.1084/jem.20052016

Yona, S., and S. Jung. 2010. Monocytes: subsets, origins, fates and functions. *Curr. Opin. Hematol.* 17:53–59. http://dx.doi.org/10.1097/MOH.0b013e3283324f80

Yona, S., K.W. Kim, Y. Wolf, A. Mildner, D. Varol, M. Breker, D. Strauss-Ayali, S. Viukov, M. Guilliams, A. Misharin, et al. 2013. Fate mapping reveals origins and dynamics of monocytes and tissue macrophages under homeostasis. *Immunity*. 38:79–91. http://dx.doi.org/10.1016/j.immuni.2012.12.001

Zhang, H.H., K. Song, R.L. Rabin, B.J. Hill, S.P. Perfetto, M. Roederer, D.C. Douek, R.M. Siegel, and J.M. Farber. 2010. CCR2 identifies a stable population of human effector memory CD4+ T cells equipped for rapid recall response. *J. Immunol.* 185:6646–6663. http://dx.doi.org/10.4049/jimmunol.0904156

Zheng, Y., P.A. Valdez, D.M. Danilenko, Y. Hu, S.M. Sa, Q. Gong, A.R. Abbas, Z. Modrusan, N. Ghilardi, F.J. de Sauvage, and W. Ouyang. 2008. Interleukin-22 mediates early host defense against attaching and effacing bacterial pathogens. *Nat. Med.* 14:282–289. http://dx.doi.org/10.1038/nm1720

Zigmond, E., C. Varol, J. Farache, E. Elmaliah, A.T. Satpathy, G. Friedlander, M. Mack, N. Shpigel, I.G. Boneca, K.M. Murphy, et al. 2012. Ly6C hi monocytes in the inflamed colon give rise to proinflammatory effector cells and migratory antigen-presenting cells. *Immunity*. 37:1076–1090. http://dx.doi.org/10.1016/j.immuni.2012.08.026